Biomedical Optics EXPRESS

Synergistic combination of near-infrared irradiation and targeted gold nanoheaters for enhanced photothermal neural stimulation

Kyungsik Eom,[1] Changkyun Im,[2] Seoyoung Hwang,[3] Seyoung Eom,[4] Tae-Seong Kim,[4] Hae Sun Jeong,[3] Kyung Hwan Kim,[2] Kyung Min Byun,[4,6] Sang Beom Jun,[3,5,7] and Sung June Kim[1,8]

[1]*Department of Electrical and Computer Engineering, Seoul National University, Seoul 151-744, South Korea*
[2]*Department of Biomedical Engineering, Yonsei University, Wonju 220-710, South Korea*
[3]*Department of Electronics Engineering, Ewha Womans University, Seoul 120-750, South Korea*
[4]*Department of Biomedical Engineering, Kyung Hee University, Yongin 446-701, South Korea*
[5]*Department of Brain and Cognitive Sciences, Ewha Womans University, Seoul 120-750, South Korea*
[6]*kmbyun@khu.ac.kr*
[7]*juns@ewha.ac.kr*
[8]*kimsj@snu.ac.kr*

Abstract: Despite a potential of infrared neural stimulation (INS) for modulating neural activities, INS suffers from limited light confinement and bulk tissue heating. Here, a novel methodology for an advanced optical stimulation is proposed by combining near-infrared (NIR) stimulation with gold nanorods (GNRs) targeted to neuronal cell membrane. We confirmed experimentally that *in vitro* and *in vivo* neural activation is associated with a local heat generation based on NIR stimulation and GNRs. Compared with the case of NIR stimulation without an aid of GNRs, combination with cell-targeted GNRs allows photothermal stimulation with faster neural response, lower delivered energy, higher stimulation efficiency and stronger behavior change. Since the suggested method can reduce a requisite radiant exposure level and alleviate a concern of tissue damage, it is expected to open up new possibilities for applications to optical neuromodulations for diverse excitable tissues and treatments of neurological disorders.

OCIS codes: (170.3890) Medical optics instrumentation; (350.4238) Nanophotonics and photonic crystals; (240.6680) Surface plasmons.

References and links

1. W. M. Grill, S. E. Norman, and R. V. Bellamkonda, "Implanted neural interfaces: biochallenges and engineered solutions," Annu. Rev. Biomed. Eng. **11**(1), 1–24 (2009).
2. J. Wells, C. Kao, E. D. Jansen, P. Konrad, and A. Mahadevan-Jansen, "Application of infrared light for *in vivo* neural stimulation," J. Biomed. Opt. **10**(6), 064003 (2005).
3. G. Bonmassar, S. W. Lee, D. K. Freeman, M. Polasek, S. I. Fried, and J. T. Gale, "Microscopic magnetic stimulation of neural tissue," Nat. Commun. **3**, 921 (2012).
4. H. Huang, S. Delikanli, H. Zeng, D. M. Ferkey, and A. Pralle, "Remote control of ion channels and neurons through magnetic-field heating of nanoparticles," Nat. Nanotechnol. **5**(8), 602–606 (2010).
5. Y. Tufail, A. Matyushov, N. Baldwin, M. L. Tauchmann, J. Georges, A. Yoshihiro, S. I. H. Tillery, and W. J. Tyler, "Transcranial pulsed ultrasound stimulates intact brain circuits," Neuron **66**(5), 681–694 (2010).
6. C.-P. Richter, A. I. Matic, J. D. Wells, E. D. Jansen, and J. T. Walsh, Jr., "Neural stimulation with optical radiation," Laser Photonics Rev. **5**(1), 68–80 (2011).
7. E. S. Boyden, F. Zhang, E. Bamberg, G. Nagel, and K. Deisseroth, "Millisecond-timescale, genetically targeted optical control of neural activity," Nat. Neurosci. **8**(9), 1263–1268 (2005).
8. X. Han and E. S. Boyden, "Multiple-color optical activation, silencing, and desynchronization of neural activity, with single-spike temporal resolution," PLoS One **2**(3), e299 (2007).
9. J. Wells, P. Konrad, C. Kao, E. D. Jansen, and A. Mahadevan-Jansen, "Pulsed laser versus electrical energy for peripheral nerve stimulation," J. Neurosci. Methods **163**(2), 326–337 (2007).
10. A. D. Izzo, C.-P. Richter, E. D. Jansen, and J. T. Walsh, Jr., "Laser stimulation of the auditory nerve," Lasers Surg. Med. **38**(8), 745–753 (2006).
11. M. G. Shapiro, K. Homma, S. Villarreal, C.-P. Richter, and F. Bezanilla, "Infrared light excites cells by changing their electrical capacitance," Nat. Commun. **3**(736), 736 (2012).

#255470 Received 10 Dec 2015; revised 20 Mar 2016; accepted 29 Mar 2016; published 31 Mar 2016

12. J. Wells, C. Kao, P. Konrad, T. Milner, J. Kim, A. Mahadevan-Jansen, and E. D. Jansen, "Biophysical mechanisms of transient optical stimulation of peripheral nerve," Biophys. J. **93**(7), 2567–2580 (2007).
13. A. R. Duke, M. W. Jenkins, H. Lu, J. M. McManus, H. J. Chiel, and E. D. Jansen, "Transient and selective suppression of neural activity with infrared light," Sci. Rep. **3**, 2600 (2013).
14. E. J. Katz, I. K. Ilev, V. Krauthamer, H. Kim, and D. Weinreich, "Excitation of primary afferent neurons by near-infrared light *in vitro*," Neuroreport **21**(9), 662–666 (2010).
15. J. D. Wells, S. Thomsen, P. Whitaker, E. D. Jansen, C. C. Kao, P. E. Konrad, and A. Mahadevan-Jansen, "Optically mediated nerve stimulation: Identification of injury thresholds," Lasers Surg. Med. **39**(6), 513–526 (2007).
16. A. C. Thompson, S. A. Wade, N. C. Pawsey, and P. R. Stoddart, "Infrared neural stimulation: influence of stimulation site spacing and repetition rates on heating," IEEE Trans. Biomed. Eng. **60**(12), 3534–3541 (2013).
17. M. M. Chernov, G. Chen, and A. W. Roe, "Histological assessment of thermal damage in the brain following infrared neural stimulation," Brain Stimulat. **7**(3), 476–482 (2014).
18. J. L. Carvalho-de-Souza, J. S. Treger, B. Dang, S. B. H. Kent, D. R. Pepperberg, and F. Bezanilla, "Photosensitivity of neurons enabled by cell-targeted gold nanoparticles," Neuron **86**(1), 207–217 (2015).
19. D. Jaque, L. Martínez Maestro, B. del Rosal, P. Haro-Gonzalez, A. Benayas, J. L. Plaza, E. Martín Rodríguez, and J. García Solé, "Nanoparticles for photothermal therapies," Nanoscale **6**(16), 9494–9530 (2014).
20. S. E. Lee, G. L. Liu, F. Kim, and L. P. Lee, "Remote optical switch for localized and selective control of gene interference," Nano Lett. **9**(2), 562–570 (2009).
21. S. A. Stanley, J. E. Gagner, S. Damanpour, M. Yoshida, J. S. Dordick, and J. M. Friedman, "Radio-wave heating of iron oxide nanoparticles can regulate plasma glucose in mice," Science **336**(6081), 604–608 (2012).
22. E. Hutter and J. H. Fendler, "Exploitation of localized surface plasmon resonance," Adv. Mater. **16**(19), 1685–1706 (2004).
23. M. E. Stewart, C. R. Anderton, L. B. Thompson, J. Maria, S. K. Gray, J. A. Rogers, and R. G. Nuzzo, "Nanostructured plasmonic sensors," Chem. Rev. **108**(2), 494–521 (2008).
24. K. Eom, J. Kim, J. M. Choi, T. Kang, J. W. Chang, K. M. Byun, S. B. Jun, and S. J. Kim, "Enhanced infrared neural stimulation using localized surface plasmon resonance of gold nanorods," Small **10**(19), 3853–3857 (2014).
25. J. Yong, K. Needham, W. G. A. Brown, B. A. Nayagam, S. L. McArthur, A. Yu, and P. R. Stoddart, "Gold-nanorod-assisted near-infrared stimulation of primary auditory neurons," Adv. Healthc. Mater. **3**(11), 1862–1868 (2014).
26. S. Yoo, S. Hong, Y. Choi, J.-H. Park, and Y. Nam, "Photothermal inhibition of neural activity with near-infrared-sensitive nanotransducers," ACS Nano **8**(8), 8040–8049 (2014).
27. J. J. Iliff, M. Wang, Y. Liao, B. A. Plogg, W. Peng, G. A. Gundersen, H. Benveniste, G. E. Vates, R. Deane, S. A. Goldman, E. A. Nagelhus, and M. Nedergaard, "A paravascular pathway facilitates CSF flow through the brain parenchyma and the clearance of interstitial solutes, including amyloid β," Sci. Transl. Med. **4**(147), 147ra111 (2012).
28. L. Xie, H. Kang, Q. Xu, M. J. Chen, Y. Liao, M. Thiyagarajan, J. O'Donnell, D. J. Christensen, C. Nicholson, J. J. Iliff, T. Takano, R. Deane, and M. Nedergaard, "Sleep drives metabolite clearance from the adult brain," Science **342**(6156), 373–377 (2013).
29. J. J. Iliff, H. Lee, M. Yu, T. Feng, J. Logan, M. Nedergaard, and H. Benveniste, "Brain-wide pathway for waste clearance captured by contrast-enhanced MRI," J. Clin. Invest. **123**(3), 1299–1309 (2013).
30. A. Blau, "Cell adhesion promotion strategies for signal transduction enhancement in microelectrode array *in vitro* electrophysiology: An introductory overview and critical discussion," Curr. Opin. Colloid Interface Sci. **18**(5), 481–492 (2013).
31. D. A. Wagenaar, J. Pine, and S. M. Potter, "Effective parameters for stimulation of dissociated cultures using multi-electrode arrays," J. Neurosci. Methods **138**(1-2), 27–37 (2004).
32. H. Kamioka, E. Maeda, Y. Jimbo, H. P. C. Robinson, and A. Kawana, "Spontaneous periodic synchronized bursting during formation of mature patterns of connections in cortical cultures," Neurosci. Lett. **206**(2-3), 109–112 (1996).
33. G. J. Brewer, J. R. Torricelli, E. K. Evege, and P. J. Price, "Optimized survival of hippocampal neurons in B27-supplemented neurobasal™, a new serum-free medium combination," J. Neurosci. Res. **35**(5), 567–576 (1993).
34. K. L. Fields, D. N. Currie, and G. R. Dutton, "Development of Thy-1 antigen on cerebellar neurons in culture," J. Neurosci. **2**(6), 663–673 (1982).
35. C. G. Dotti, R. G. Parton, and K. Simons, "Polarized sorting of glypiated proteins in hippocampal neurons," Nature **349**(6305), 158–161 (1991).
36. W. S. Lee, M. K. Jain, B. M. Arkonac, D. Zhang, S.-Y. Shaw, S. Kashiki, K. Maemura, S.-L. Lee, N. K. Hollenberg, M.-E. Lee, and E. Haber, "Thy-1, a novel marker for angiogenesis upregulated by inflammatory cytokines," Circ. Res. **82**(8), 845–851 (1998).
37. S. Tandon, N. Kambi, and N. Jain, "Overlapping representations of the neck and whiskers in the rat motor cortex revealed by mapping at different anaesthetic depths," Eur. J. Neurosci. **27**(1), 228–237 (2008).
38. M. Brecht, M. Schneider, B. Sakmann, and T. W. Margrie, "Whisker movements evoked by stimulation of single pyramidal cells in rat motor cortex," Nature **427**(6976), 704–710 (2004).
39. X. D. Wang, O. S. Wolfbeis, and R. J. Meier, "Luminescent probes and sensors for temperature," Chem. Soc. Rev. **42**(19), 7834–7869 (2013).
40. A. J. Verkhratsky and O. H. Petersen, "Neuronal calcium stores," Cell Calcium **24**(5-6), 333–343 (1998).

#255470 Received 10 Dec 2015; revised 20 Mar 2016; accepted 29 Mar 2016; published 31 Mar 2016

41. N. Kato, T. Tanaka, K. Yamamoto, and Y. Isomura, "Distinct temporal profiles of activity-dependent calcium increase in pyramidal neurons of the rat visual cortex," J. Physiol. **519**(2), 467–479 (1999).

1. Introduction

Among a variety of external sources employed to modulate a neural membrane potential, electrical stimulation has been the gold standard due to good controllability and high reliability [1]. However, as electrical stimulation suffers from limited spatial precision by inherent electric field spreading and inevitable invasiveness for charge delivery [2], alternative strategies such as magnetic [3,4], mechanical [5], and optical [2,6–8] methods have been suggested to modulate neural activities in central and peripheral nervous systems.

As one of the most promising neuro-modulation techniques, optical stimulation has increasingly gained popularity in the last decade, allowing contact-free and electrical artifact-free stimulation with a spatiotemporally precise control [2,6–8]. In particular, optogenetic method uses light to excite or inhibit genetically targeted neural cells with a high spatiotemporal resolution [7,8]. Although it is an excellent tool for preclinical breakthroughs, optogenetics is still unavailable in clinical use owing to controversial issue of genetic manipulation in human. On the other hand, infrared neural stimulation (INS) enables us to control neural activities by delivering infrared light energy into the target neural cells without genetic modification [2,6,9,10]. While the underlying mechanism is not clear yet, it has been hypothesized that infrared light can excite or inhibit neural cells depending on the thermal gradient at the cell membrane [4,6,11–14]. However, conventional INS incorporating infrared wavelength in the range of 1450 – 2200 nm has been in trouble with tissue damage due to strong water absorption [15]. Although tissue damage is different for the stimulation strategy and condition [16], possible tissue damage due to light absorption by a bulk tissue is still existing [15,17]. A visible light is also available [18], but its low skin transparency can restrict the potential for non- or minimally invasive neural stimulation. Near-infrared (NIR) light with a longer penetration depth is thus considered appropriate for an efficient temperature rise in the target tissue since cells are more transparent in this wavelength [19].

Metallic or magnetic nanoparticles interacting with electromagnetic waves have been utilized to modulate cellular functions through a conversion of external optical [20] or magnetic [4,21] energy into a thermal heat. Illuminating gold nanorods (GNRs) at their resonant wavelengths leads to efficient light absorption and local electromagnetic field enhancement, finally realizing a plasmonic nanoheater [22–24]. Since plasmonic nanoheaters can efficiently elevate local temperature, INS combined with GNRs has a potential for improving an optical activation or inhibition of neuronal metabolisms [18,24–26] while avoiding tissue damage by excessive heating. Previously, we presented that an optical neural stimulation using NIR light incorporating plasmonic nanoheaters injected in a proximity of neuron cells could significantly enhance the neural responses of a rat sciatic nerve *in vivo* [24]. However, unconjugated nanoparticles might be ineffective when they are washed off by extracellular fluid flow. Strongly bound nanoparticles to the target are more critical in central nervous system (CNS) because body fluid such as cerebrospinal fluid (CSF) in CNS flows continuously through living cells to dump out the metabolic wastes [27–29]. While membrane localization of nanoparticles was previously reported [26], for example, GNRs were designed to have a positive charge on the surface to bind with a negatively charged plasma membrane of neuronal cell, a target-specific binding for selective neuromodulation is not feasible.

Hence, in this study, an advanced NIR stimulation is suggested based on surface-modified nanoheaters of GNRs that are targeted to neural cell membrane. Bound GNRs based on antigen-antibody complex can offer not only a strong affinity but also a target-dependent specificity that could be used in cell-specific targeting of GNRs. Here, GNRs are attached to a membrane of cultured hippocampal neuron, and the neural responses evoked by NIR irradiation are measured. The stimulation threshold and the neural unit responses such as stimulation efficiency and latency are compared with the result of a conventional NIR stimulation without GNRs. Moreover, we demonstrate that the proposed stimulation strategy

#255470 Received 10 Dec 2015; revised 20 Mar 2016; accepted 29 Mar 2016; published 31 Mar 2016

is feasible for evoking a movement of rat whisker *in vivo*. It is expected that our study could provide new possibilities for optical neuromodulation and treatment of neurological disorders.

2. Experimental methods

2.1 Cell culture

Hippocampi are dissected from Sprague-Dawley rat embryos (E19) under sterile conditions in accordance with the animal research guidelines of Use Committee of the Institute of Laboratory Animal Resources at Ewha Womans University (IACUC No. 15-045). Cells are dissociated using 5% trypsin-EDTA for 15 mins prior to trituration and then are plated at 1,800 cells/mm^2 on multi-electrode arrays (MEAs, MultiChannel systems, Reutlingen, Germany) coated with poly-L-lysine (P4707, Sigma-Aldrich, St. Louis, MO, USA) [30,31]. Culture of hippocampal cells for 2 to 3 weeks is found to provide tightly synchronized periodic bursting, which is advantageous for distinguishing spontaneous activity from optically evoked activity [31,32]. The culture medium refers to the method by Brewer et al.; Neurobasal medium (NEUROBASAL Medium, 21103, GIBCO, CA, USA) with B-27 supplement (17504-044, GIBCO, CA, USA), 2 mM glutamax (35050, GIBCO®, CA, USA), and antibiotics (15240, Life technologies, Carlsbad, CA, USA) [33]. Cultures are kept in an incubator at 36.5°C at 5% CO_2.

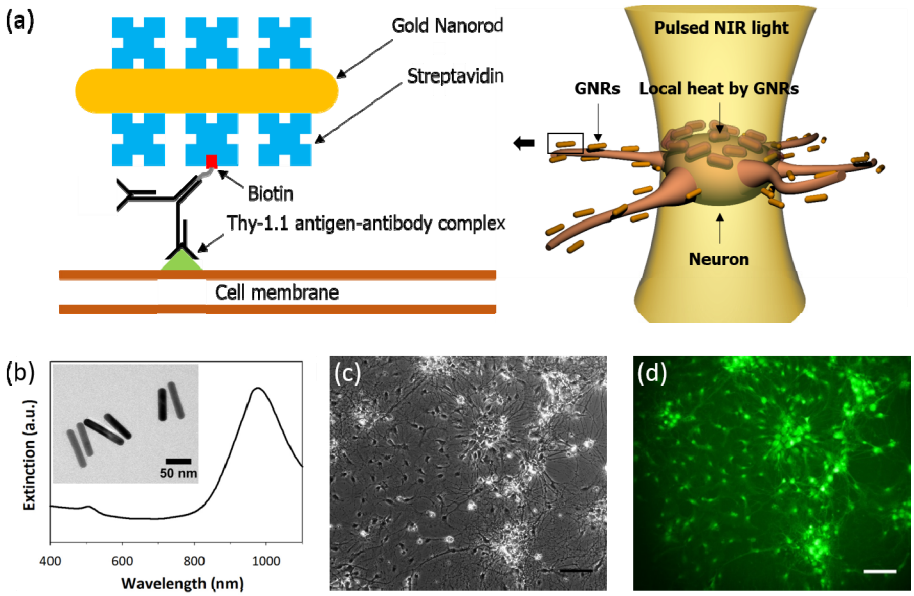

Fig. 1. Optical stimulation of neuron using surface-modified GNRs. (a) Streptavidin coated gold nanorods (GNRs) are delivered to the neuron by biotinylated anti-Thy-1 antibody that bind to an epitope from external neuronal membrane. Localized heat from strongly bound GNRs could elicit neuronal depolarization. (b) TEM image reveals that average geometric dimensions of GNRs are 80.4 nm in length and 15.3 nm in width. Optical extinction spectrum of GNRs shows a longitudinal absorption peak at λ = 977 nm. (c) The phase contrast microscope image shows a typical hippocampal neural cell after 18 days *in vitro*. Cell bodies as well as axons can be distinguished morphologically. (d) After neuronal membrane is tagged by biotinylated anti-Thy1.1 antibody, streptavidin-coated GNRs are incubated to form a strong binding with biotinylated antibody. Biotinylated FITC is used to observe the distribution of streptavidin-coated GNRs. Scale bar, 100 μm in (c) and (d).

2.2 Conjugation of GNRs to neuronal cell membrane

Biotinylated antibody is employed to target the neuron cell membrane combined with streptavidin-conjugated GNRs (Fig. 1(a)). As it has been well known that Thy-1 antigen

#255470 Received 10 Dec 2015; revised 20 Mar 2016; accepted 29 Mar 2016

exists as a glycosylphosphatidylinositol (GPI)-anchored protein on the surface of neuron cells [34,35], the neuronal surface is tagged by biotinylated anti-Thy-1 antibody. GNRs covered with streptavidin are intended to bind with biotinylated antibody which is located on the surface of neuron so that GNR-mediated heat could effectively raise the temperature of the neuronal membrane.

At first, structural and optical properties of GNRs are characterized. Streptavidin-coated GNRs (C12-10-980-TS, Nanopartz Inc., Loveland, CO, USA) with a concentration of 3.4×10^{13}/mL are prepared. The size and shape of GNRs are characterized by transmission electron microscopy (TEM, Libra 120, Carl Zeiss, Germany) and extinction spectrum is measured using a wide-band spectrophotometer (UV-1800, Shimadzu, Japan) to find a surface plasmon resonance peak. As shown in Fig. 1(b), average values of the length and width of GNRs are measured as 80.4 nm and 15.3 nm, respectively, resulting in the aspect ratio equal to 5.3. For elongated GNRs with two plasmonic resonance modes, as a longitudinal mode at $\lambda = 977$ nm along the long-axis is more prominent for photothermal effect than a transverse mode at $\lambda = 505$ nm, pulsed infrared laser with a wavelength of $\lambda = 980$ nm is chosen as a light source of NIR simulation. While extinction peak of GNR is adjustable in a wide range of visible and NIR wavelengths depending on the aspect ratio [20], the use of resonant wavelength in NIR band is considered advantageous in terms of heat generation in a deep tissue [19].

In order to verify whether streptavidin-conjugated GNRs are well bound to the cell membrane, the distribution of GNRs is visualized according to the following processes: Cultured neuron cells 18 days *in vitro* (Fig. 1(c)) are fixed in warm 4% paraformaldehyde for 15 mins and washed with PBS three times. Subsequently, without perfusion of Triton X-100 which is a routine immunocytochemistry protocol, BSA is applied to prevent a non-reactive binding. Cells are then washed with PBS before incubating in biotinylated anti-Thy-1 antibody (554896, BD Biosciences, San Jose, CA, USA) diluted by 1:100. After washing with PBS three times, streptavidin-coated GNRs (5.1×10^{11}/mL) are added to form antibody-GNRs complex. Cells are washed three times and incubated with biotinylated FITC (B-1370, Life Technologies, Carlsbad, CA, USA) for staining. Using an inverted microscope (IX71, Olympus, Tokyo, Japan), we visualize the distribution of GNRs. Strong FITC fluorescent signal found at the surface of hippocampal neurons implies a high avidity to anchor the GNRs proximal to the neuronal membrane, avoiding diffusion of GNRs away from the target neurons (Fig. 1(d)).

In the following *in vitro* experiments, we determine an incubation time to minimize an internalization of GNRs by living samples and to form a strong antigen-antibody reaction for stable attachment of GNRs. From the previous reports, we find that anti-Thy-1.1 antibody generally requires at least an hour to bind to the cell membrane [34,36]. Hence, we set an incubation time of antibody-conjugated GNRs at 2 hours to realize a strong and stable attachment.

2.3 Stimulation and recording system for cultured hippocampal neuron in vitro

Figure 2 illustrates the schematic of neural stimulation and recording system based on MEAs. Cultured hippocampal neurons are exposed to 980 nm laser pulses generated from fiber-coupled laser diode. At the end of optical fiber, collimator and focusing lens are mounted to yield a focused NIR beam spot with a diameter of 400 μm. Optically evoked neural responses are recorded via MEA electrical recording system consisting of pre-amplifier, band-pass filter, and data acquisition board.

Cultures incubated in the MEA are transferred to a recording system and visualized through an inverted microscope to obtain a bright field image. We use a glass MEA (MultiChannel systems) with 30 μm diameter titanium nitride for electrode, silicon nitride for insulation layer and transparent indium tin oxide for contact pads and tracks. MEA is composed of 59 electrodes laid out in a rectangular grid with 200 μm inter-electrode spacing. Signals are pre-amplified (× 1100), filtered in a bandwidth from 1 Hz to 3 kHz by MEA 1060-Inv-BC amplifier (MultiChannel Systems), and digitized using MC-Card (MultiChannel Systems). Neural signal recordings are pre-triggered for 100 ms prior to the electrical/optical

#255470 Received 10 Dec 2015; revised 20 Mar 2016; accepted 29 Mar 2016; published 31 Mar 2016

stimulation and end until 1 s. All the recorded data are analyzed using an off-line software MC-Rack (MultiChannel Systems) and filtered digitally (70 Hz highpass filter).

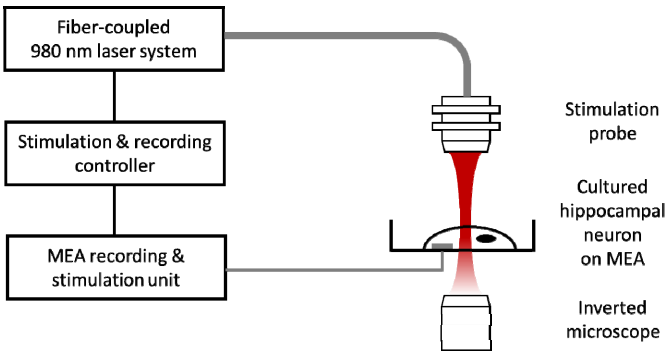

Fig. 2. Experimental setup of stimulation and recording for cultured hippocampal neuron. Neuron is cultured on MEAs and pulsed NIR light is irradiated by fiber-coupled laser diode. Stimulus-triggered neural activities are recorded from the MEA. For electrical stimulation and recording, stimulus is delivered through the one of electrodes and stimulus triggered neural responses are recorded from the rest of the electrodes in MEA.

Prior to optical stimulation, electrical stimulation and recording are performed in advance to check the neural response to the stimuli. We produce an anodic-first biphasic current stimulation pulse of current level of 20 μA and a width of 200 μs per phase using stimulus generator STG-4008 (MultiChannel Systems). 10 stimulation pulses with a period of 60 s are delivered and the evoked responses of cultured neuron cells are recorded. Subsequently, laser diode with a wavelength of 980 nm which is directly coupled to the 400 μm core optical fiber with numerical aperture equal to 0.14 (Pearl P14 Series, nLIGHT, Vancouver, WA, USA) is used to optically stimulate a neuron. Laser driver PLD 10K-CH (Wavelength Electronics Inc., MT, USA) is used to manipulate the stimulation parameters of the laser. Accurate positioning of NIR stimulation is controlled by monitoring a visible guiding beam through optical microscope. After determining a stimulus area, 10 stimulation pulses with a period of 60 s and a pulse width of 400 μs are delivered and optically evoked responses are recorded. Prior to optical stimulation, the culture medium is replaced with 1.5 mL of artificial cerebrospinal fluid (aCSF, composition (in mM): 124 NaCl, 4.5 KCl, 1.2 NaH_2PO_4, 26 $NaHCO_3$, 1 $MgCl_2$, 2 $CaCl_2$, 10 Glucose with 15 mins 5% CO_2 bubbling) and maintained in the incubator (36.5°C, 5% CO_2) for 15 mins for stabilization.

2.4 Stimulation and recording system for rat motor cortex in vivo

Since photothermal stimulation with NIR light can be optimal for many *in vivo* applications due to high tissue penetration and lower absorption by hemoglobin as compared to a visible light [19], combination of NIR irradiation and cell-targeted GNRs are employed to stimulate neurons in a rat motor cortex of whisker region *in vivo* to evoke whisker movement. For *in vivo* INS experiments, Spraque-Dawley rat aged 9 weeks (~290 g) is initially anesthetized with intraperitoneal injection of urethane (200 mg/kg). The rat is then placed in a stereotaxic apparatus (51600, Stoelting Co, Wood Dale, IL, USA), and incision is made in the scalp. Using the bregma as the reference point rectangular craniotomy is performed. Antibody-conjugated gold nanorods are prepared and injected to the vibrissae motor cortex *in vivo*. Injection is conducted using 75 μm diameter glass capillary injection tip (SBB-75X-00, Sunlight Medical, Jacksonville, FL, USA) mounted in a microprocessor-controlled injection system (Nanoliter 2010, World Precision Instruments, Sarasota, FL, USA). Antibody tagged gold nanorods are filled in the glass capillary tip and injected at the rate of 23 nL/s at a position of anteriorly 2.9 mm, laterally 1.5 mm, and 1.0 mm in depth relative to bregma.

Optical stimulation is carried out using above mentioned fiber-coupled laser diode. Fiber is positioned ~2 mm above the brain where nanoparticles are injected (Fig. 3). The

#255470 Received 10 Dec 2015; revised 20 Mar 2016; accepted 29 Mar 2016

stimulation parameters are 50 ms train of fifteen 1.5 ms pulses at 300 Hz with a pulse intensity of 128 mJ/cm^2 which are determined based on the stimulation parameter of intracortical microstimulation (ICMS) [37,38]. The pulse duration of the optical stimulus is selected as 1.5 ms at which whisker movement is maximized when it is varied in the range from 0.5 ms to 2.0 ms. A train of stimulus set is given every two seconds. After optical stimulation, electrical stimulation (66.7 ms train of twenty monophasic, negative, 0.2 ms pulses at 300 Hz with amplitude of 2.4 mA) is delivered through tungsten microelectrode where light is delivered to check the functionality after optical stimulation [37,38]. We videotape whisker movement using CCD camera (C920, Logitech, Lausanne, Switzerland) before and after optical stimulation. Whisker movement is measured by reference to image pixels at fixed x positions in the (x, y) coordinate frame of the camera (to a first approximation, whisker movement is primarily in the y direction). The angular movement of whisker of interest is quantified in a frame-by-frame analysis using MATLAB.

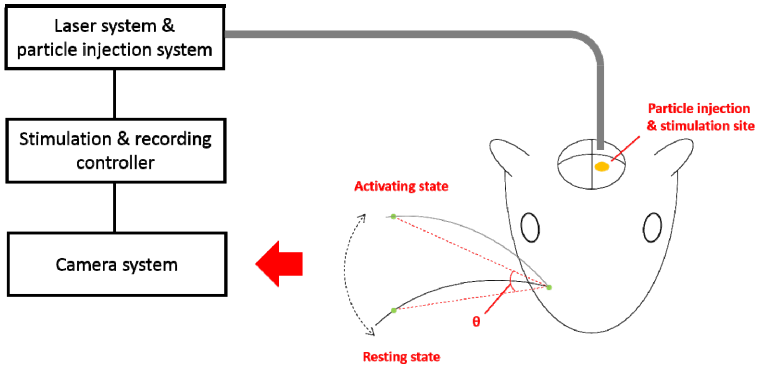

Fig. 3. Experimental setup of optical stimulation and recording system for rat vibrissae motor cortex *in vivo*. GNRs are injected (anteriorly 2.9 mm, laterally 1.5 mm, and 1.0 mm in depth relative to bregma, indicated by a yellow ellipse) prior to the optical stimulation. Whisker trajectories monitored by CCD camera, angle change between the resting and activating states (indicated by two dotted lines) are extracted.

3. Results and discussion

3.1 NIR stimulation of cultured hippocampal neuron using cell-targeted GNRs

Before demonstrating a neural response associated with NIR stimulation and cell-targeted GNRs, spontaneous activities of cultured neural cells are monitored. Array-wide synchronized burst activities are obtained and a time interval between bursts is presented by an inter-burst interval (IBI) histogram. In Fig. 4(a), spontaneous burst firing with an average interval of 10.8 s is measured, which indicates that cultures are in the state of development of synaptic connection [32]. Electrical stimulation is delivered to the electrode where strong spontaneous activities are recorded. For electrical stimulation, a neural response is defined as a spike with a peak lower than −12 μV while neglecting the stimulation artifact that appears around 0 s. The first evoked neural response tends to appear in 10-20 ms after the electrical stimulus (Fig. 4(b)). When stimulus efficiency is defined as a percentage of the number of stimuli evoking action potentials to the total number of applied stimuli, the stimulus efficiency of electrical stimulation is measured to be 100%, verifying a high reliability of electrical neural stimulation. Moreover, from the post-stimulus time histogram (PSTH) shown in Fig. 4(c), the majority of action potentials occur no later than 150 ms and the latency, time to get the maximum spikes after stimulus, is 25 ms.

#255470 Received 10 Dec 2015; revised 20 Mar 2016; accepted 29 Mar 2016

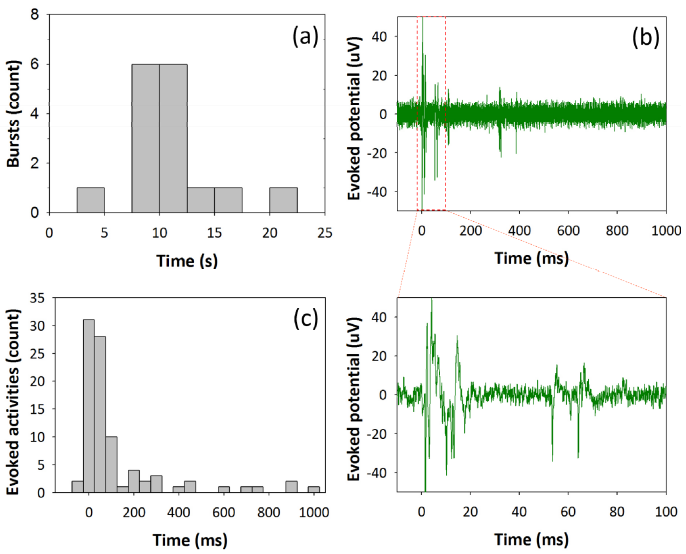

Fig. 4. Characteristic of neural response upon electrical stimulus. (a) An inter-burst interval histogram without electrical stimulation reveals that burst fires every 10.8 s. (b) Evoked action potentials after electrical stimulation (Stimulus parameters: anodic-first biphasic current stimulation pulse, current amplitude of 20 μA, and a width of 200 μs per phase) show neurons fire immediately after stimulus. (c) A post-stimulus time histogram to show the temporal distribution of electrically evoked action potentials. Neurons respond to the electrical stimuli having latency (time to get the maximum spikes after stimulus) of 25 ms.

Having verified the cellular excitability upon external stimuli, optical stimulation without cell-targeted GNRs is performed. Cell medium is replaced with 1.5 mL of aCSF and culture is maintained in the incubator (36.5°C, 5% CO_2) for 15 mins. Optical pulse is delivered to the neuron for 400 μs every 60 s while increasing its stimulus intensity to evoke neural depolarization. Note that, the data without cell-targeted GNRs in this study are assumed to include both cases for untreated GNRs and no GNRs. From the previous publication, the photosensitivity results for untreated GNRs and no GNRs showed insignificant difference in the effect of optical stimulation on DRG neurons [18]. It was also demonstrated that perfusion of fresh buffer rapidly washed the nanoparticles out, abolishing their effect. Even without active washing, diffusion of gold nanoparticles away from the neuron cell was sufficient to abolish the optical responses.

The stimulation threshold is defined as the minimum radiant exposure required to evoke action potentials with first three consecutive laser pulses while having stimulus efficiency over the 50%. While stimulating without cell-targeted GNRs, stimulation threshold level is determined to be 46.9 mJ/cm^2 and stimulus efficiency is measured to be ~80%. In Fig. 5(a), neural responses are synchronized to optical stimulus showing that optically evoked neural activities range over several hundreds of milliseconds. Due to such a wide-spreading firing distribution, the latency of PSTH is increased to 265 ms, which is approximately ten times bigger than the result of electrical stimulation of 25 ms (Fig. 5(b)).

Subsequently, highly localized GNRs-mediated optical stimulation of neuron is performed by conjugating GNRs to antibodies that specifically bind to external membrane proteins. Neuronal cells are tagged with surface-modified GNRs by replacing aCSF with a cell culture medium containing a mixture of biotinylated anti-Thy-1 antibody (3.3 μg/mL) and streptavidin-conjugated GNRs (2.3×10^{11}/mL). After 2 hrs of incubation, cells are washed three times thoroughly with aCSF and incubated at 36.5°C and 5% CO_2 for 15 mins for stabilization. The neural activities are evoked as shown in Fig. 4(c). The GNR-tagged neurons elicit enhanced stimulus efficiency up to 90% at the threshold intensity of 30.1 mJ/cm^2, which is notably lower than the neurons without conjugation of GNRs. Also, the neural activities are

#255470 Received 10 Dec 2015; revised 20 Mar 2016; accepted 29 Mar 2016

evoked with a reduced latency of 95 ms as presented in PSTH compared to optical stimulation without cell-targeted GNRs (Fig. 5(d)). Together, these data show that functionalized GNRs bound to the neuronal membrane enable fast optical neuronal depolarization with low laser intensity while displaying high resistance to washout. When GNRs are tightly bound to the membrane, it is likely that direct change in membrane capacitance and/or rapid opening of temperature-sensitive ion channels allows for a relatively faster depolarization than NIR stimulation without cell-targeted GNRs. Especially, localized NIR stimulation by GNRs bound to the target neuron may contribute to minimization of off-target environmental heating and increase an excitation efficiency for robust stimulation [18].

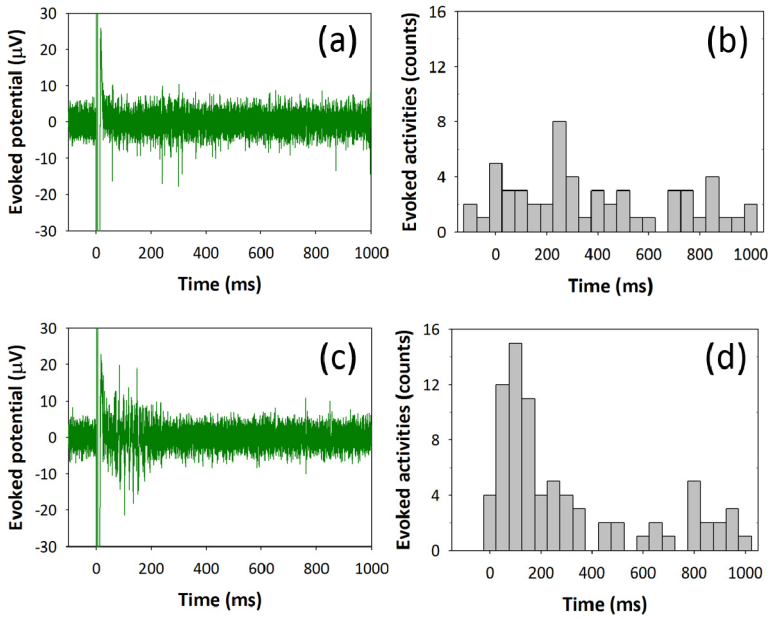

Fig. 5. Characteristic of neural response upon optical stimulus with and without cell-targeted GNRs. (a) Evoked action potentials after optical stimulation without cell-targeted GNRs show neurons are sensitive to optical stimulus and trigger neural activities at the threshold intensity of 46.9 mJ/cm^2. (b) A post-stimulus time histogram to show the temporal distribution of optically evoked action potentials. Neurons respond to the optical stimuli having latency (time to get the maximum spikes after stimulus) of 265 ms. (c) Evoked action potentials after optical stimulation with cell-targeted GNRs show neurons fire right after stimulation with small temporal jitter. Laser threshold intensity used to evoke neural response is 30.1 mJ/cm^2 which is about the half of the laser intensity stimulating without cell-targeted GNRs. (d) A post-stimulus time histogram to shows reduced latency of 95 ms.

3.2 Cortically controlled whisker movement using NIR stimulation and cell-targeted GNRs

Antibody-conjugated GNRs are injected into whisker region of a rat motor cortex and trains of optical pulses are delivered to the target tissue while measuring a whisker movement. In Fig. 6(a), we find that NIR stimulation with cell-targeted GNRs facilitates a response of whisker oscillation. No significant whisker angle change is observed and an exact value of simulation threshold could not be found when stimulating the motor cortex with no aid of GNRs. While the experimental results for verifying the reproducibility are not shown here, we find that overall trends are consistent, although there is slight difference in the amplitude of angle difference and the delay time to initiate the movement. To check the functionality and the cell viability of stimulation site in motor cortex, optical stimulation is followed by electrical stimulation. Strong stimulus-locked whisker movement is electrically evoked, implying that whisking function remains intact during the courses of NIR stimulation as shown in Fig. 6(b). Although whisker movement triggered by optical stimulation is fairly

#255470 Received 10 Dec 2015; revised 20 Mar 2016; accepted 29 Mar 2016; published 31 Mar 2016

weak and slow compared to the results of electrical stimulation, whisker movement in the presence of GNRs clearly shows an enhancement comparing to the case without GNRs.

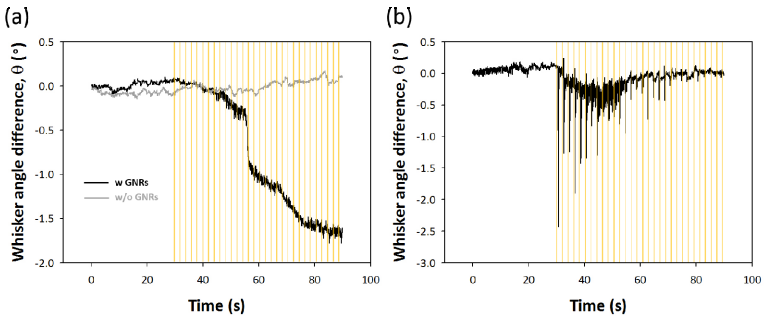

Fig. 6. Whisker movement evoked by optical and electrical stimulation of rat vibrissae motor cortex *in vivo*. (a) Whisker trajectories according to optical stimulation with and without antibody-conjugated GNRs. Optical stimuli (indicated by yellow line) are applied with train of fifteen pulses at 300 Hz with pulse duration of 1.5 ms and a period between the trains of 2 s. (b) Whisker trajectories when electrical stimuli are applied with 66.7 ms train of twenty monophasic, negative, 0.2 ms pulses at 300 Hz with amplitude of 2.4 mA.

3.3 Local temperature change induced by NIR stimulation

For optically evoked action potentials, it has been hypothesized that temperature elevation localized at a neuron cell can depolarize the membrane potential by directly changing membrane capacitance or opening temperature-sensitive ion channels [4,11]. Thus, local heat generation by GNRs and rapid heat dissipation is important for spatiotemporally precise stimulation of neuronal activity. In order to measure the temperature change induced by NIR stimulation combined with GNRs, FITC bound to GNRs is employed because its fluorescent intensity is proportional to the temperature change of surrounding medium [4,39]. Therefore, the temperature dependence of biotinylated FITC is characterized in aqueous solutions. While the solution containing FITC is slowly heated in a custom-made chamber equipped with a temperature controller (TC02, MultiChannel systems), the fluorescent intensity is recorded with high sensitive CCD camera (Zyla 5.5 sCMOS, ANDOR, UK) and the average fluorescent intensity in a region of interest is obtained during temperature change. Figure 7(a) shows a linear decay of normalized fluorescent intensity with an increasing temperature. Linear regression analysis shows that fluorescent intensity as a function of temperature change is determined to be $y = -0.0047x + 1.002$ and $R^2 = 0.9852$. Fit line obtained is used to estimate the time-varying temperature characteristic.

After finding the relation between temperature change and fluorescent intensity, we measure the temperature change due to the laser exposure. We enclose 10 μL solution containing biotinylated FITC (1 mg/mL) bound to GNRs (1.7×10^{11}/mL) between a microscope slide glass and a cover glass (Marienfeld-Superior, Lauda-Königshofen, Germany). Laser beam with a radiant exposure 190 mJ/cm^2 and a pulse width of 400 μs is irradiated on the thin sandwiched sample and fluorescent signals are collected during 10 ms before and 100 ms after the onset of optical stimulation with a frame rate of 500 frames per seconds. Fluorescent intensity of each image is averaged and converted into average temperature. When a solution containing biotinylated FITC bound to GNRs is irradiated by the laser, the temperature rapidly increases up to 5°C within 20 ms and returns to the base level room temperature immediately (Fig. 7(b)). On the other hand, no significant temperature change occurs in the solution without GNRs. This indicates that local temperature increases by illuminating GNRs can induce a selective and localized heating of neuron cells depending on the presence of GNRs and contribute to a rapid and spatiotemporally precise optical stimulation of neuron cells.

#255470 Received 10 Dec 2015; revised 20 Mar 2016; accepted 29 Mar 2016; published 31 Mar 2016

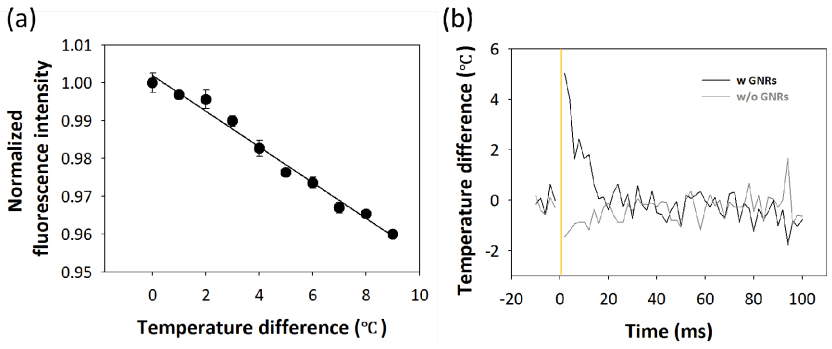

Fig. 7. Characterization of local heat generation by GNRs. (a) Temperature dependence of fluorescent intensity of biotinylated FITC shows a linear decrement of normalized fluorescent intensity upon temperature increment. (b) Temperature profiles are measured from temperature-sensitive fluorescent dyes before and after illuminating laser (indicated by yellow line) in solutions with and without GNRs. Temperature is monitored by capturing average fluorescent intensity with a frequency of 500 Hz.

3.4 Discussion

We discuss that the latency measured while stimulating neurons without cell-targeted GNRs is delayed compared to the latency measured in the case of cell-targeted GNRs (Fig. 5). It is possible that the latency is delayed by the prolonged activation of neurons due to the residual heat near the cells after bulk tissue heating. Otherwise, there may exist different underlying mechanisms between optical stimulation with and without GNRs. When stimulating neuron with cell-targeted GNRs, GNRs that bound to cell surface generate localized heat to triggers neural activities. However, without GNRs, high laser intensity is needed to stimulate the neurons which cause bulk heating of cells. We speculated that the bulk heating could induce transient membrane capacitance change of not only the cell surface membrane but also the membrane of intracellular organelles. Some intracellular organelles such as endoplasmic reticulum or mitochondria, where calcium is stored, dynamically participate in generation of intracellular calcium signals enhancing neuronal activities [40]. The light-induced activation of intracellular organelles can trigger intracellular signaling via the increase of intracellular calcium concentration. This hypothesis is consistent with the delayed latency because the intracellular calcium signaling is known to be slow compared to inward calcium influx through voltage-gated calcium channels activated by action potentials [41].

4. Conclusion

We demonstrated that cell-targeted GNRs convert NIR irradiation into the rapid and local temperature elevation which can trigger physiological changes in the cell membrane evoking neural activities of cultured neurons and rat motor neurons *in vivo*. Once antibody-conjugated GNRs are attached to the cell membrane, strongly bound GNRs are found to be effective for photothermal NIR stimulation as it can provide a lower stimulation threshold and a faster neural activation compared to the case of optical stimulation without an aid of GNRs. *In vivo* experiment of rat whisker movement verified the possibility of modulating the neural cells and tissues by combination of NIR stimulation and targeted GNRs.

While the underlying mechanism of NIR stimulation associated with GNRs is not clear yet, recent evidences have shown that any heat-related physiological change seems a key factor. Shapiro et al. have shown that transient heat variance near the cell membrane induces a change in membrane capacitance, leading to a membrane depolarization even without an aid of ion channels [11]. Huang et al. also showed thermal activation of temperature sensitive ion channel (e.g. TRPV1) can trigger action potentials in cultured neurons [4]. Our subsequent study will be more focused on the analysis of NIR stimulation mechanism in a quantitative way.

#255470 Received 10 Dec 2015; revised 20 Mar 2016; accepted 29 Mar 2016

Acknowledgments

This work was supported by the Brain Korea 21 Plus Project, the Department of Electrical and Computer Engineering, Seoul National University in 2015 and by a grant to CABMC (Control of Animal Brain using MEMS Chip) funded by Defense Acquisition Program Administration (UD140069ID). This study was also supported by engineering-dentistry interdisciplinary research grant jointly funded by college of engineering and college of dentistry, Seoul National University, by the National Research Foundation of Korea (NRF) grants funded by the Korea government (MEST) (2014R1A2A2A09052449 and 2015R1A5A1037656), and by CISS as GFP (CISS-2012M3A6A6054204) and NRF-2014R1A1A1A05003770.

#255470 Received 10 Dec 2015; revised 20 Mar 2016; accepted 29 Mar 2016; published 31 Mar 2016